ФІЗИКА І ХІМІЯ ТВЕРДОГО ТІЛА
Т. 10, № 3 (2009) С. 707-714

PHYSICS AND CHEMISTRY OF SOLID STATE
V. 10, № 3 (2009) P. 707-714

PACS 85.40.HP

ISSN 1729-4428

G.M. Mladenov, K.J. Vutova, E.G. Koleva

Computer Simulation of Electron and Ion Beam Lithography of Nanostructures

Institute of Electronics at Bulgarian Academy of Sciences
72, Boul. Tzarigradsko shosee, Sofia 1784, Bulgaria
e-mail: mladenov@ie.bas.bg

In this paper a review of the authors results on mathematical modeling of the processes at electron or ion beam lithography of nanostructures is presented. Our Monte Carlo simulation tools for electron and ion exposures are successfully applied for the energy deposition calculation at electron or ion lithography of resist layers. At ion lithography electronic energy losses of penetrating electrons are responsible for the usable resist modification. Development models are different for used resists in nanolithography and are of special interest. Examples of linear and nonlinear (multi-ciphered) dependencies of the solubility rate on exposure dose are given. Some examples of numerical simulation results for 2D and 3D resist profiles obtained using electron and ion lithography are presented.

Key words: electron lithography, ion lithography, polymer resists, chemically amplified resists, non-organic resists, exposure, development, resist modification, latent image, developed resist profile

Стаття поступила до редакції 07.02.2009; прийнята до друку 15.06.2009.

I. Introduction

The lithography is the key technology for fabrication of new generation electronic devices, now in the nano-dimension region. Next steps in nano-electronics, being now in the range of 45 nm critical dimension of the produced microprocessors and memories, are connected with improvement and optimization of micro-structuring technologies and before all - of the electron and ion lithography. There the resist-profile-relief simulation using computer models play increasingly a important role. Only correct selection of the exposure and development conditions can ensure the necessary higher resolution and the desired resist profile and dimensions.

In this paper some peculiarities of the electron and ion lithography as prospective methods for nano-structuring through the features of the used algorithms for adequate description of the created images and the resist edge profiles after lithography development are discussed.

II. Exposure modeling

2.1. Deposited energy in the case of electron beam lithography simulation.

In many computer codes the penetration of irradiating electrons in the polymer layer is calculated utilizing Monte Carlo method (our algorithm is given in [1]). Random numbers are used for assuming the scattering atom type from the composition probability function, for choice of the azimuthally component of the scattering angle and for estimation of electron scattering-angle-components in the meridian-plane from the concrete value of the differential cross-section for the elastic collision of penetrating electron determined by the

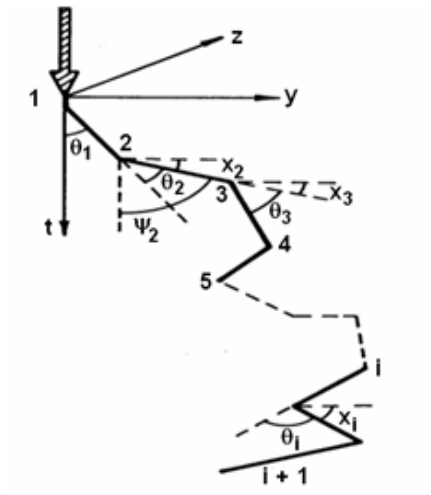

Fig. 1. Trajectory of a penetrating particle in material. The points of scattering of penetrating particle are given with a number. There are shown also the respective components of the scattering angle.

next elastic collision with the selected atom, chosen in the same way (from probability determined by sample composition) is estimated using another random numbers. This distance, shown as straight line between two collisions is a part of the estimated value of the penetrating electron mean free path. The electron trajectory is assumed as a zigzag path, consisting of straight-line segments with definite length - Fig.1. The places of elastic collisions of penetrating electron with sample atoms are the points between these distances. The energy losses, as result of the inelastic electron collisions with atom electrons (or mainly with the collective outer-bands electrons of the solid sample) are calculated on the base of Bethe stopping-power theory. In this way one could know energy of the penetrating electron and deposited energy losses in a small local region of sample. The calculation continues until the previously chosen cut-off conditions (lowest energy of penetrating electrons, electron positions out of the sample volume) are satisfied. The calculated energy loss is written in a matrix in the respective resist space position. After calculation of enough much trajectories (usually 10 000) these discrete data presents the spatial distribution of the absorbed energy in the resist for delta-function of the electron incidence.

So the point exposure energy deposition function (EDF) is determined as a histogram function of the radial distance from the direction of the electron penetration and from the depth of resist layer. Often this function is called also proximity function because determines proximity effect – a interaction of the exposures doses at irradiation of big amount of image points on sample surface, due to the scattering of the penetrating electrons in longitudinal direction. The proximity effect requires high accuracy of calculation of point exposure absorbed energy distribution at large radial distances from the point of beam incidence. Increasing the simulating trajectory numbers slowly improves the statistics in this region. A Monte Carlo methodology and a corresponding computer program are developed for transformation of discrete absorbed energy distribution (histogram) in analytic function [2]. This provides a better data, from the statistical point of view, for the further calculation.

The EDF(r) usually consists from two components, as this could be shown in Fig.2. These components are two Gaussian functions with maximal values $\mathbf{c_f}$ and $\mathbf{c_b}$ and dispersions $\boldsymbol{\beta_f}$ and $\boldsymbol{\beta_b}$. The maximal values $\mathbf{c_f}$ and $\mathbf{c_b}$ are coefficient of the weight of so called forward scattering component and back scattering component of the deposited energy in resist at irradiating the studied surface point. In the case of simulation of absorbed energy distribution in cylindrical coordinates instead Cartesian - ones it is possible to simulate a beam incidence inclined to the resist surface [3]. There was applied a procedure for re-calculation of the free path and electronic stopping power when a penetrating electron crosses the interfaces in multilayer structures [4].

Another energy deposition function, noted as SEDF, evaluated at exposure of a pixel (a beam spot) or a single element of irradiated image (a line, a rectangle etc.) is calculated as convolution of the point exposure energy distribution (EDF) and the distribution function of the

Rutherford shielding potential of the concrete scattering atom. There the concrete free-movement-distance to the

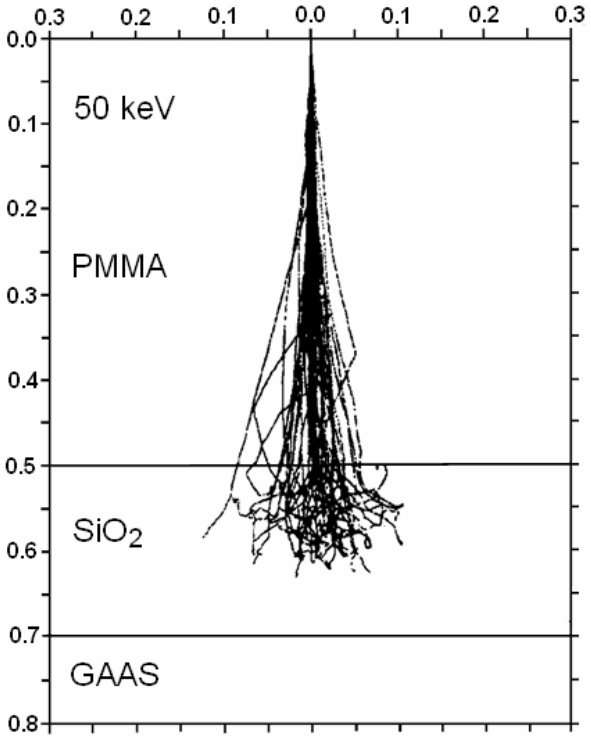

Fig. 5. Trajectories of ions (50 keV protons) penetrating in PMMA of thickness 0,5μm on SiO_2 top layer of SiO2/GaAs substrate.

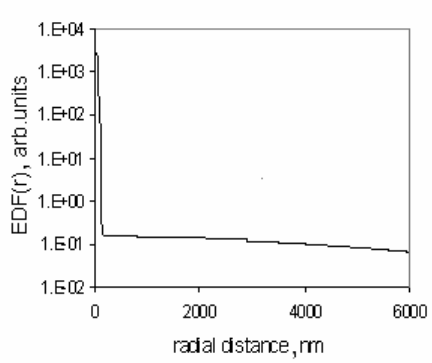

Fig. 6. Monte Carlo simulation data for the EDF(r) calculated at the resist/substrate interface in the case of ion beam exposure with He+ ions with energy 100 keV are shown.

beam electrons in the irradiated spot or simple section of image. Due to usual presentation of the point exposure distribution function as sum of Gaussians (some time an additional exponent could be used in the intermediate region) the adsorbed energy due to exposure of a single element of exposed image can be calculated using the tabulated Error function that saves the computer resources.

2.2. Deposited energy in the case of ion beam lithography simulation.

The accelerated ions has changed it sown charging state during the movement through the irradiated sample, going to be neutralized or to come to highest charged state as a function of the penetration ion velocity. Stopping power and trajectory of penetrating

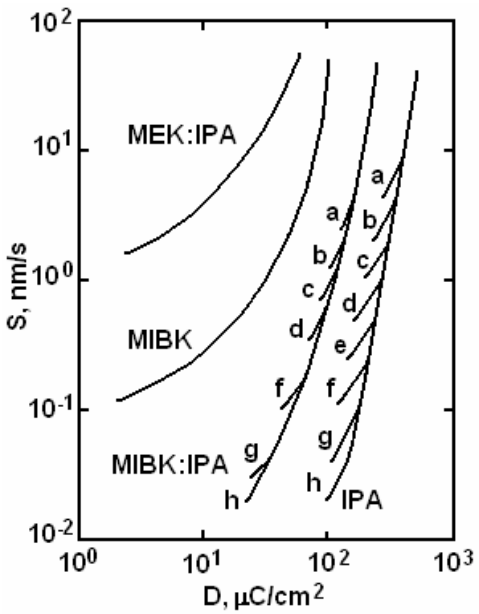

Fig. 7. Dependance of solubility (development) rate S versus exposure dose D of PMMA (polymethyl methacrylate) and various developers. The resist thickness is 5000 nm, the development time is (for multi-ciphered curves –i.e. case of nonlinear development): a-15s, b-30s. c-60s, d-120s, e-240s, f-480s, h-1920s.

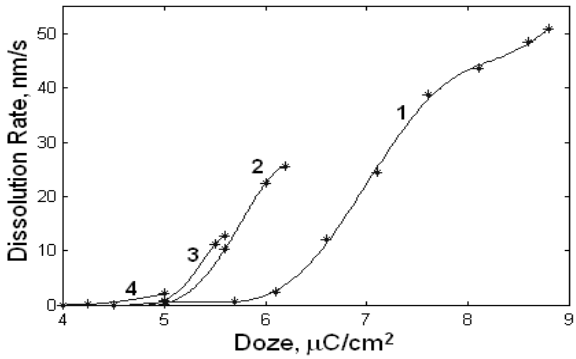

Fig. 8. Experimental characteristics of solubility rate vs dose of electron exposure of CAMP6 chemically amplified resist at various times of development: 1 – 15 s; 2 – 30 s; 3 – 60 s; 4 – 360 s.

particles in the material at ion bombardment have been well understood, due to the progress of ion implantation and others ion technologies. Our Monte Carlo program is described also in [1] and is a member of TRIM family. The program structure is analogical to the electron simulation code, described shortly above. The major difference is that energy transfer is executed by two types of energy losses: (i) nuclear stopping power, due to penetrating particle collisions with the sample atoms and (ii) electronic stopping power, due to penetrating projectile collisions with the electrons in the bombarded material.

In our earlier applications of the computer code [5] were evaluated the ranges and energy losses of various ions in polymethil methacrylate (PMMA). The values of projected and lateral ranges have been calculated for various penetrating particles and energies. The displaced secondary atoms in cascades are taking in account.

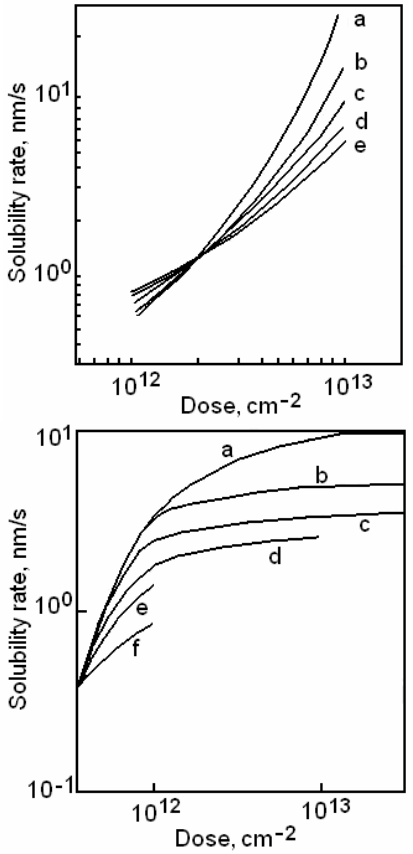

Fig. 9. a) Non-linear S(D) for 80 kV He+ irradiation of PMMA (M=675 000)using MIBK:IPA=1:1 at 20°C. The development times are: a-30s, b-60s, c-90s, d-120s, e-150s;
b) PMMA sensitivity, measured versus ion dose S(D) for 120 keV Ar^+ . The development conditions are as in the case of Fig.9a.

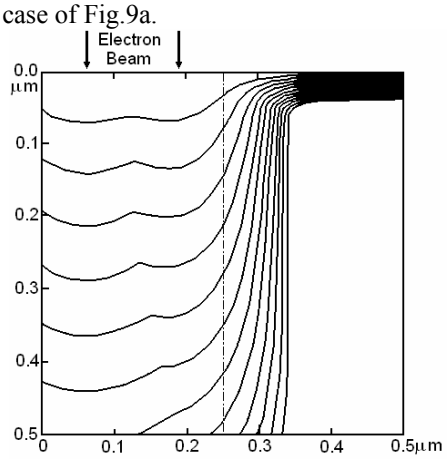

Fig. 10. Simulated EBL profiles in a 0,5 μm developed isolated line(half of the profile is shown). Resist thickness is 500 nm; substrate - 80nm Cr thin film on thick SiO_2. The time intervals are 10s. Dose of exposure -80 μC/cm^2. The exposure electron beam have Gaussian distribution with σ =50nm.

By such calculations one can see that the scattering and lateral dispersion of the penetrating particles through resist are small for the ions, which are of three orders of magnitude heavier than the electrons (Fig.5 and Fig.6). Therefore the proximity effects that are the major problem in the electron beam lithography (EBL) is minimal in the ion beam lithography (IBL).

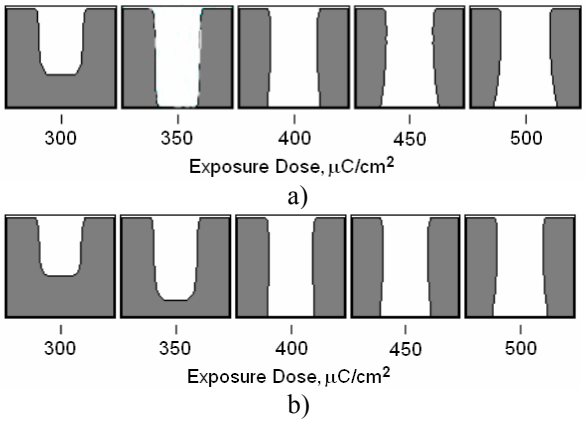

Fig. 11. Simulated resist profiles for the central part of the central line of a layout consists of numerous 250 nm wide long parallel lines spaced by 500 nm for a wide range of exposure dose. The resist used is 0.4 μm PMMA and e-beam energy is 50 keV The substrates are: a) YBCO/STO substrate; b) Si substrate.

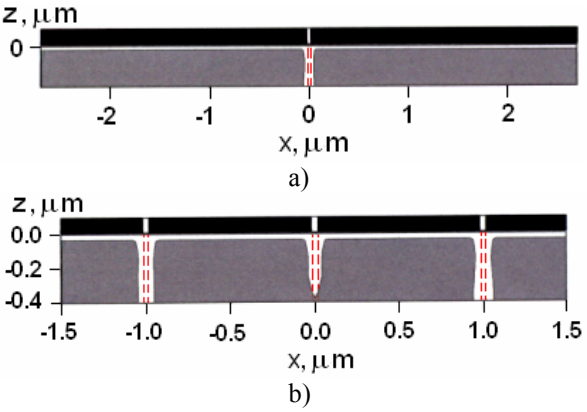

Fig. 12. a) Simulated resist profiles in the case of 30 nm wide isolated long line at a dose of 0.35 μC/cm^2, resist thckness 0.4μm (PMMA/S i), development time - 5 min The beam width is presented by the white band in the symbolic black mask on the top, the substrate is not shown. The developed line profile shapes differ from the beam exposed area.
b) Two dimensional simulated resist profiles for three lines for different exposure doses (0.325μC/cm^2 , 0.25 μC/cm^2, and 0.4μC/cm^2) by 100 keV He ions. The incident beam width is presented also by the white band in the symbolic black mask on the top, the substrate is not shown. The developed line profile shapes differ from the beam exposed area.

From the results, obtained in ref. [6,7] and confirmed or accepted by few tens authors has been assumed that electronic energy losses are responsible for observed solubility modification in ion beam lithography using polymer resists. The nuclear stopping power has obtainable effect on the solubility modification in the case of heavy low energy ion modification [8] at non-linear development rates (see bellows).

Fig. 13. EBL - 3D resist profiles at 50 keV of exposed image consists one 30 nm wide line and four 0.8 x 0.8 μm^2 squares. The image dimensions between components are limited by the proximity effect. After development the minimal possible distance between line and squares is 635 nm and the line width - 410 nm predicted by computer simulation.

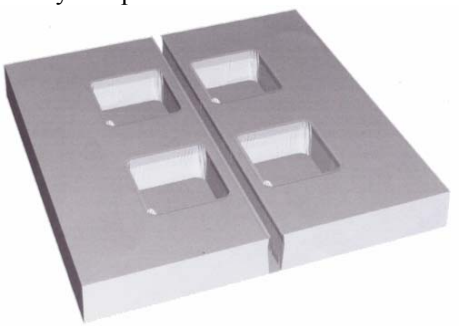

Fig. 14. IBL - 3D resist profiles after exposure with 100 keV He^+ ion beam. The exposed image consists the same dimensions of the exposed line and the squares (namely one 30 nm wide line and four 0.8 x 0.8 μm^2 squares). After development the distance between line and squares is 185 nm.

Fig. 15. 3D resist profiles of the exposed microstructures (parallel lines) at exposure with ion beams of parameters as in the Fig.14. The external proximity effect is not observed.

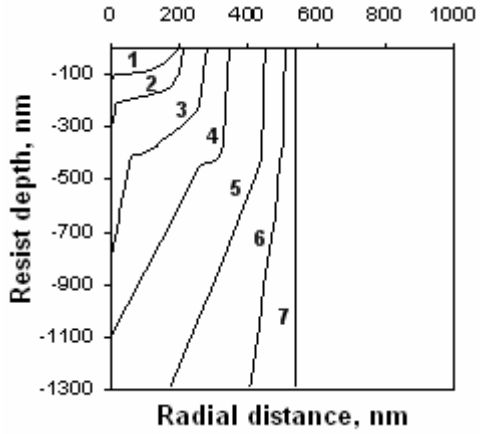

Fig. 16. Simulated development profiles of an isolated 500 nm line created in CAMP6 resistfilm on Si for different times of development in OPD 262-developer (PEB 120^{o}C, 60s): 1-17s, 2-19s, 3-21s; 4-22s, 5-23s, 6-25s, and 7-27s(half of the developed profiles is shown).

III. Modeling of resist development

3.1. Solubility rate dependencies on the exposure dose.

The goal of the computer simulation of the processes in EBL and IBL is prediction of the resist profile and the image dimensions of the developed exposed microstructure. During the exposure of the samples, covered by a sensitive to irradiation layer there are a modification of the local solubility rate of this resist and as a result could be observed the developed image as removed and non-removed areas of the treated resist layer. Respectively to solubility changes of irradiated areas one could distinguish positive-tone or negative tone resists. The first important step of the modeling of the changes of the resist thickness is to transfer the absorbed energy distribution in resist due to exposure in distribution of the local solubility (in the case that is the development) rate. Due to different chemistry composition of utilized resists and to increasing requirements on the exactness of the predicted profiles in various dimension ranges of the developed images (as example: in one micron, submicron, sub 0,250 or less than 50 nm orders of the image critical dimensions) the models used in computer simulation of profile dimensions and of its edge are different and concrete choice of model and fitting parameter used there are a most critical step of this prediction. The integral-circuit-manufacturers use concrete and limited number of resists and any available simulation tool, keep as confidential the obtained fitting parameters and applied approximations.

In the nanoelectronic device technology there are three type more important resists: (i) one component organic positive tone resist represented by polymethil methacrylate (PMMA), (ii) chemically amplified resists represented by SAL, CAMP and ARCH types, as well as (iii) the inorganic resist hydrogen silsesquioxane (HSQ). The experimental data on the development rates vs. exposure doses of these resists (experimentally for argument of this dependence instead the energy density-i.e. absorbed energy in one volume unit is easily as approximation to obtain by contrast curves that dependence on exposure dose as argument) together with the data for used developer and development conditions are given in ref. [9].

In the case of PMMA the conversion of the absorbed energy distribution in the resist to the solubility rate is based on radiation modification of the polymer molecular weight in studied point of the resist [10]. At chosen couple resist – developer, conditions of development, resist initial molecular weight, exposure dose and radiation yield (efficiency, measured as the number of scissions per electron-volt absorbed energy), a definitive development rate could be estimated. The dissolution rate in these conditions of unexposed resist is another parameter used in simulation. Often the changes of the absorbed energy density distribution on the resist deep are neglected and only its radial (lateral) distribution is used at simulation. The dependence of solubility rate on exposure dose for various developers is shown on Fig. 7. From these curves one can see that sensitivity could be increased at loss of the developed structure contrast. Also two types of resist solubility were distinguished: linear and nonlinear solutions. Examples of the same multi-ciphered dependencies of solubility rate on exposure dose are shown for other resists (Fig.8) and at ion irradiation (Fig.9a and Fig.9b). Reasons are various: role of interface layer with another solubility rate than bulk resist material, time dependence of developer penetration into the solid resist, role of nuclear energy losses that deteriorate polymer structure at ion modification of resist material.

Then the resist removal in that case is simulated as movement of interface between solid polymer and liquid developer. The developer – resist interface is a function of time. For a short developing time each evaluating point from the moving development contour (or plane in the case of 3D simulation) advances along the normal to the profile with its local solubility rate. There a procedure to increase the contour (plane) accuracy by increasing the evaluating point number in the parts with significant curvature is applied. Cubic (or bi-cubic) splines are used to describe the developed profiles [1,2].

In the case of chemically amplified resists (CARs) there are two or three polymer components one of which is a radiation active component (RAC). During exposure of RAC is generated a radiation product and a diffusion of that radiation product take place during thermal processe, called post-exposure bake (PEB) applying in this case. In the CARs this radiation product (an acid) working as catalytic agent modifies the base component solubility rate. The models for the conversion of the solubility rate through the RAC concentration and the solubility rate modification products are described in [11-13].

In these models various descriptions of the diffusion and loss of the catalytic species (acid) and of the kinetics of de-protection (switching resist solubility) reaction; the need of molecular development rate model incorporating the surface changes (retardation or elevation) of the development rate are the reasons for the serious problems. Additional reasons for a loss of the accuracy are (i) the variations in utilized resist and developer pairs; the different PEB times and temperatures; (ii) the different procedures of the extraction the experimental parameters; (iii) the geometry changes of parameter values; (iv) the batch to batch alteration between the resist material properties. That causes a need of final experimental calibration of the model parameter set, used in such a simulation. A question in ref. [14] is: whether to evaluate each reaction quantitatively using experimental and theoretic values of too many factors or to build one simplified model based on simple experimental calibration procedures? This model could represent only main steps: the absorbed energy distribution in the resist after exposure, the modification of de-protected polymer distribution during post exposure bake (PEB) and on base of the evaluation of solubility rate in various resist points to simulate resist profile.

For the CAR type CAMP6 a nonlinear solubility process was observed [13]. Therefore simple mathematical relation between the development rate and the exposure dose for the resist profile evaluation was not applicable. Time dependant calculation scheme and multi-ciphered experimental dependencies of the solubility rate on the exposure dose are used for an adequate simulation of the development kinetics of the resist profile [13, 14].

A spin coated inorganic resist, observed in the last time is attractive – the hydrogen silsesquioxane (HSQ) [15]. This is negative tone resist. It provides high thermal stability, good gap-filling and crack free adhesion to metal film surfaces. HSQ is oligomer composing of a caged silsesquioxane along with a linear Si-O network. A standard thermal cure is performed to convert the cages to the highly cross-linked network through reaction in silicon hydride (Si-H) parts of the chains. The same curing reaction could also be accomplished through electron irradiation. The structure transition drastically decreases the dissolution rate of matrix in an aqueous solvent performing a negative tone relief pattern. Furthermore HSQ can also be utilized in a bi-layer lithography scheme due to its high etch resistance properties where the patterns are transferred through a sub-layer using a reactive ion etching. Etch resistance of HSQ is excellent. Resist drying could be optimized effectively by replacing the rinsing liquid with a supercritical fluid [16]. Optimal doses depend upon beam energy, desired resolution and film thickness. Using instead the mixture of salt and alkali a development in an aqueous mixture of NaOH alkali and NaCl salt enhances the contrast. Contrast values as high as 3-10 and resolution better than 10 nm were achieved for electron irradiation[17-20] and 20 nm level at proton irradiation [21]. Increasing of temperature of development to 45^{o}C also is increasing the contrast and resolution. The extremely high resolution of HSQ is obtained at cost of higher than in the CARs exposure doses. The contrast and line-wall roughness (line-wide fluctuations) is much lower than contrast in traditional chain scission PMMA due to the oligomer nature of HSQ.

The simulation of HSQ resist profile dimension and shape of edge is analogically to the one component resist PMMA only one could use solubility rate vs. exposure dose S(D) given in [9], created by our experimental data as regression equation.

IV. SIMULATION RESULTS

On the Fig.10 is shown computer simulation of evolution of the developed in the positive tone resist PMMA profile of a 2D semi-cross-section of an isolated line. The exposure beam irradiated surface of developing trench in lines (points) situated on 62,5 nm and 187,5 nm from the central axis of the irradiating area. The beam is of a Gaussian distribution with dispersion 50 nm. The time interval between two developed profiles is 10 s. The resist thickness is 500 nm. Dashed line noted desired width of the line (trench) of 0,5 μm. Total development time is 2 min.

On the next Fig.11 the role of the atomic weight of the substrate on the optimal dose at EBL is demonstrated. Developed 2D profiles in the resist are shown. They are taken of central line (trench) from a great number of long-parallel-lines exposed with various doses. The width of each line of the exposed layout is 250nm and distance between lines is 500 nm. The doses of exposure are in the range of 300-500 μC/cm^2 as they are written bellows each developed profile. The resist is PMMA and the exposure is by electrons with energy 50 keV. On the Fig.11a are given the case of substrate composed by a film of yttrium-barium cooper-oxide $YBa_2Cu_3O_{7-x}$ deposited on substrate of $SrTiO_2$ monocrystal . On Fig.11b is shown the case of Si substrate. The increased quantity of back scattering electrons in PMMA, generating from the heavies substrate (YBCO on STO) in a comparison with these electrons from Si substrate, that have lower atomic number and atomic mass provide higher absorbed energies from back-scattered electrons. This lead to providing higher development rates and the optimal development (where the profiles are with nearly vertical walls) is executed at lower doses. In the case of PMMA on YBCO / STO the optimal dose evaluated by this simulation is 350 μC/cm^2 instead of 400μC/cm^2 for the case of PMMA on Si .

On Fig. 12a is shown 2D simulated resist profile for a line developed in PMMA resist after exposure with 100keV He+ ion beam. The beam width (image width equal to 30nm) is presented by the white band in the symbolic black masks on the top of shown structures in Fig.12a and 12b. The developed line width is 101 nm at the top of the resist layer. This width is 106 nm at the Si substrate, while it is 96nm at the narrowest part of the developed line cross-section. This extension of the developed line width is similar to the internal proximity effect in case of EBL. On Fig.12b are given results of simulation of IBL of 2D profiles of three isolated developed lines(trenches) exposed with 100 keV He^+ ions. The exposure doses are 0.325μC/cm^2, 0.25 μC/cm^2 and 0.4μC/cm^2 respectively for line sat x=-1μm, x=0 μm and x=1μm. The beam width of 30 nm is represented by white band in symbolic black mask as well as with dashed lines in the developed in the positive resist profiles. Development time is 5 min. It can be see difference between developed resist profiles. The good developed trench is obtained at exposure ion dose of 0.325μC/cm^2 situated at x=-1 μm. The line in the sample center is not enough developed. The resist profile of line exposures with dose of 0,4 μC/cm^2 is wider near the bottom. The simulated total thickness decrease is 7.3% at these conditions.

On Fig. 13 and Fig. 14 are shown computer simulated 3D structures, developed in resist of one line and 4 rectangles, situated at minimum-possible distance one of other. In the EBL case (Fig.13) proximity effect is seen as a increase of widths and more round shapes of rectangle segments. The distances between IBL developed segments of the similar image are shorter. This is due to lack of external proximity effect at IBL. This is demonstrated too in Fig.15 where a great number of parallel lines are simulated after developing in positive resist.

More interesting is the case of development in a nonlinear (i.e. multi-ciphered and time dependent) couple of resist and developer. In ref. [13, 14] is done computer simulation of EBL of the chemically amplified resist CAMP6 using OPD-262 developer. From the experimental dependence S(D) for that resist and developer, presented on Fig. 8, one can see a slow development rate at low exposure doses and a sharp increase of the resist removal at higher doses (and various development times). In ref.[13 ,14] is shown micrographs of the developed line (trench) observed at different values of the development time. The central part of the exposed lines beginning to appear only after a development time of 15 s and the developed trench with vertical walls is seen after 30 s. Fig. 16 shows the time evolution of the simulated development profiles for a line in CAMP6 using OPD-262 developer. The developed profiles are obtained by computer simulation for the following conditions: a single line with a 500 nm width in 1.7 μm thick CAMP6 (initial resist thickness) on Si, the incident electron energy is 30 keV, the beam diameter is 500 nm. From the initial resist thickness of 1.7 μm the remaining thickness was 1.3 μm due to a resist-film thickness loss of non-exposed areas after PEB and development. Higher dissolution rates in the zones with applied higher exposure doses lead to creating a central region of the exposed structure with rapid removal of the resist (see curves 1,2 and 3 on Fig. 16). At the centre of profile one can see a fragment with nearly vertical walls and bottom, which comes very quickly to the interface resist/silicon substrate. The resist profiles calculated using our model – curves 5,6 and 7 are then extended towards the periphery of the developing structure, obeying the necessary delay time at the boundaries of the different zones. The last profiles – curves 6, and 7 are with almost vertical walls correspond qualitatively to the experimentally obtained shapes of the rest of the developed trenches.

Conclusions

In the current work a short description of the main steps of the simulation models for EBL and IBL and the peculiarities of the developed MC models are described and discussed. Using the simulation tools the effects of irradiated particles – electrons and ions, exposure dose, dense patterns and nature and characteristics of the

development process are discussed in order to extract the necessary values for high resolution patterning. From the obtained results it is seen that the developed algorithms describe adequately the processes during EBL and IBL. The created simulation tools permit to predict with good accuracy the critical dimensions and profiles of the developed pattern are presented.

The simulations of IBL structures demonstrate the potential of ion lithography to be considered as one of the main competitors for further improvement of fabrication performance of the new generations of nano-electronic devices. The simulation results are very useful during optimization of concrete EBL and IBL technological processes for complex layouts in the nano-dimensional microstructuring.

Acknowledgements

The study is supported by the Bulgarian National Fund "Scientific Investigations" through contract Bg-Ukr-01-193.

Mladenov G.M. – corresponding member of BAS, Prof. Dr. Sc. of Phys., Head of Laboratory Physical problems of electron technologies at Institute of electronics – Bulgarian Academy of Sciences;
Vutova K.J. – professor, Dr.Sc.of Phys;
Koleva E.G. – Assoc.Professor, Ph.D.

[1] G. Mladenov, K. Vutova. Computer simulation of exposure and development in electron and ion lithography // *Proceedings of St.Petrsburg Electrotechnical University*, issue "*Solid State Physics and Electronics*", ed. B. Kalinikos, publisher "SPbGETU LETI", St.-Petersburg, Russia,**1**, pp.133-173 (2002).

[2] K. Vutova, G. Mladenov. Modeling of exposure and development processes in electron and ion lithography // *Modelling and Simulation in Material Science and Engineering*, **2**, pp.239-254 (1994).

[3] Y.M. Geueorguiev, G. Mladenov, D. Ivanov. Monte Carlo Simulation of Inclined Incidence of Fast Electrons to Solid // *J.Vac.Sci.Technol.*B **14**, p.2462 (1996).

[4] Y.M. Geueorguiev, G.Mladenov, D.Ivanov. Monte Carlo Simulation of Electron Beam Exposure Distribution in the Resists on Structures with High Tc Superconducting Thin Films // *Thin solid Films* 251, p.67 (1994).

[5] G.M. Mladenov, M. raun, B. Emmoth, J.P. Biersack. Ion Beam Impact and Penetration of Polymethil Methacrylate // *J.Appl. Physics*, **58**, p.2534 (1985).

[6] G.M. Mladenov, B. Emmoth. Polymethil Methacrylate Sensitivity Variation versus the Electronic Stopping Power at Ion Lithography Exposure // *Appl.Phys.Letters,* **38**, pp.1000-1002 (1981)

[7] G.M.Mladenov, B.Emmoth, M.Braun. Some effects at ion modification of polymethiyl methacrylate // *Vacuum*, **34**, pp.551-553 (1984).

[8] K. Vutova, G. Mladenov. Sensitivity, contrast and development process in electron and ion lithography // *Microelectronic Engineering*, **57-58**, pp.349-353 (2001).

[9] G. Mladenov, E. Koleva, K. Vutova, I. Kostic, V.S pivac. Resists for electron beam nanolithography

[10] // *Electronica and Electrotehnika,* **44** (5-6) pp.16-23 (2009) (Scientific and technical journal Published in Sofia, Bulgaria by CEEC)

[11] K. Murata, E. Nomura, K. Nagami,T. Kato, H**.** Nakata. Experimental profiles of resist patterns in electron-beam lithography // *J.Vac.Sci.Technol.* **16** (6), pp.1734 -1738 (1979).

[12] N. Tam, H. Liu, C. Spason, A. Neureuther. A statistically based model of electron-beam exposed, chemically amplified resist // *J.Vac.Sci.Technol.* B **9**(19), p.3362 (1991).

[13] N. Glezos, G.P. Patsis, I. Raptis, P. Argitis. Application of a reaction-diffusion model for negative chemically amplified resists to determine electron-beam proximity correction parameter // *J.Vac.Sci.Technol.* B **14** (6), pp.4252-4256 (1996).

[14] K. Vutova, E. Koleva, G. Mladenov. Some peculiarities of resist-profile simulation for positive-tone chemically amplified resists in electron beam lithography // *J.Vac.Sci.Technol.* B **27**(1), p.52-57 (2009).

[15] K. Vutova, E. Koleva, G. Mladenov, I. Kostic, T. Tanaka, K. Kawabata. A simulation model for CAR CAMP6 // *Microel. Engineering* doi: 10.1016/j.mee.2008.11.010

[16] H. Namatsu, T. Yamaguchi, N. Nagase, K. Yamazaki, K. Kurihara. Resist Materials Providing Small Line-Edge Roughness // *Microel. engineering*, **41/42**, p. 333 (1998)

[17] H**.** Namatsu, Supercritical resist drying for isolated nanoline formation, // *J.Vac.Sci.Technol.* B **19,** 2709 (2001).

[18] J.K.W. Yang and K.K. Berggren. Using high-contrast salty development of hydrogen silsesquioxane for sub-10-nm half-pitch lithography // *J. Vac. Sci. Technol.* B **25** p.1071-1023, (2007)

[19] L. Millard, G. Cunde, S. Tedeso, B. Dal′zotto, J. Voucher. HSQ hybrid lithography for 20 nm CMOS device development // *Microel.Engineering*, **62-62** , pp.755-761 (2002)

[20] F.C.M.J.M. van Delft, J.P. Weterings, A.K. van Langen-Suurling, H.Rumijn. HSQ novolac bilayer resist for high aspect rathio nanoscale EBL // *Journ. Vac.Sci.Technol.B*, **18** (6) , pp.3419-3423 (2000)

[21] A.T. Jamieson, C.G. Willson, Y. Hsu, A.D. Brodie. HSQ bilayer resist process for low voltage EBL // *Proc.SPIE* **4690**, pp.1171-1179 (2002).

[22] J.A. VAN Kan, A.A. Bettiol, F. Watt. Hydrogen silsesquioxane a next generation resist for proton beam writing at the 20 nm level // *Nuclear Instruments and Methods in Phys.Res.* B 260, pp.396-399 (2007).